Mathematical Biosciences and Engineering

MBE, 21(4): 5556–5576.
DOI: 10.3934/mbe.2024245
Received: 10 February 2024
Revised: 22 March 2024
Accepted: 26 March 2024
Published: 02 April 2024

https://www.aimspress.com/journal/MBE

Research article

Multiscale distribution entropy analysis of short epileptic EEG signals

Dae Hyeon Kim†, Jin-Oh Park†, Dae-Young Lee and Young-Seok Choi*

Department of Electronics and Communications Engineering, Kwangwoon University, Seoul 01897, South Korea

* **Correspondence:** Email: yschoi@kw.ac.kr.

† These authors contributed equally to the work.

Abstract: This paper proposes an information-theoretic measure for discriminating epileptic patterns in short-term electroencephalogram (EEG) recordings. Considering nonlinearity and nonstationarity in EEG signals, quantifying complexity has been preferred. To decipher abnormal epileptic EEGs, i.e., ictal and interictal EEGs, via short-term EEG recordings, a distribution entropy (DE) is used, motivated by its robustness on the signal length. In addition, to reflect the dynamic complexity inherent in EEGs, a multiscale entropy analysis is incorporated. Here, two multiscale distribution entropy (MDE) methods using the coarse-graining and moving-average procedures are presented. Using two popular epileptic EEG datasets, i.e., the Bonn and the Bern-Barcelona datasets, the performance of the proposed MDEs is verified. Experimental results show that the proposed MDEs are robust to the length of EEGs, thus reflecting complexity over multiple time scales. In addition, the proposed MDEs are consistent irrespective of the selection of short-term EEGs from the entire EEG recording. By evaluating the Man-Whitney U test and classification performance, the proposed MDEs can better discriminate epileptic EEGs than the existing methods. Moreover, the proposed MDE with the moving-average procedure performs marginally better than one with the coarse-graining. The experimental results suggest that the proposed MDEs are applicable to practical seizure detection applications.

Keywords: epilepsy; seizures; electroencephalogram; entropy; distribution entropy (DE); multiscale distribution entropy (MDE)

1. Introduction

Over 65 million individuals worldwide have epilepsy, and 10% of the population will have at least one seizure in their lifetime [1,2]. Epilepsy is characterized by a persistent predisposition to epileptic seizures, which are transient neurological manifestations triggered by anomalous and excessive neuronal activity in the brain [3]. Seizures caused by epilepsy can result in fractures, automobile accidents, isolation, anxiety, cognitive decline, and mortality [4]. Thus, developing a prompt diagnosis is essential for preventing morbidity and mortality due to epilepsy. As per the clinical recommendations pertaining to epilepsy surgery, the epileptic seizure focus refers to the specific region inside the cortex from which the seizures originate [5].

Standard diagnostic methods include electroencephalography (EEG), computed tomography (CT), positron emission tomography (PET), and functional magnetic resonance imaging (fMRI). EEG is a non-invasive recording of the electrical activity of the brain measured by electrodes placed on the scalp [6]. EEG has been recognized as one of the best medical tests which assist in epilepsy diagnosis because EEG exhibits high temporal and poor spatial resolution [7].

Since abnormal discharges (e.g., spikes) are generated by the synchronous discharges of large groups of neurons, it has been established that epileptic EEG recordings exhibit high complexity and nonlinearity [8–10]. In addition, EEG patterns are highly nonstationary and differ for each individual and seizure states, including normal, ictal (during seizure), and interictal (between seizures). The onset of clinical epileptic seizures is denoted by the manifestation of pertinent symptoms that are readily discernible in EEG recordings. Latency pertains to the interval that elapses between the expert-identified onset of an EEG recording and the detection system's detection of a seizure. Therefore, an algorithm that accurately detects the onset of epileptic seizures in real-time with a reduced latency period is increasingly advantageous for patients [11,12].

Considering the properties of EEGs, numerous nonlinear analysis methods, particularly entropy, have been widely adopted for distinguishing epileptic EEG patterns [9]. Entropy measures the complexity of nonlinear signals and systems by quantifying the randomness of their patterns [13]. Recently, a number of entropy methods have been widely used to detect ictal EEG or classify interictal and ictal EEG recordings. Approximate entropy (ApEn) assesses how often new patterns emerge that are different from those that have already appeared in the data [14,15]. As a modification of ApEn, sample entropy (SampEn), the negative logarithm of the conditional probability, has gained a lot of attention in analyzing various physiological signals [16]. Fuzzy entropy which uses various fuzzy membership functions to mitigate the threshold effect, has been developed [17]. Permutation entropy is a concept introduced to measure the complexity of a time series by analyzing the patterns of order relations between its values rather than the values themselves [18]. Since conventional entropy methods depend on long-term EEG recordings, it is problematic to detect epileptic seizures online using short-term EEG recordings. In addition, most entropy measures lack practical use because they rely on predefined parameters.

In addition, versatile entropy measures consider the irregularity of a time-series rather than the complexity of the system, resulting in inconsistency. Considering the entropy of temporal fluctuations, the multiscale entropy (MSE) measure has been proposed to address the inconsistency [19]. MSE is comprised of a coarse-graining procedure and SampEn evaluation in order to exploit long-range correlation. The coarse-graining procedure generates a new time-series by setting a window with a scale factor size over the original time-series and then averaging the values in each window. The

multiscale versions of conventional entropy measures have been developed inspired by MSE. However, because coarse-graining reduces the length of a time-series, it may result in an unstable evaluation of entropy values at large scales [13,20]. Thus, the use of an overlapping moving-average has been presented for the computation of MSE [13,21]. More recently, capable multiscale-based nonlinear dynamic indicator have been developed and shown their effectiveness in various applications [22,23].

Recently, DE has been introduced [24]. DE uses probability density estimation to take into account the inherent information of the distance between vectors in state space. DE is less sensitive to the length of a time-series and parameters that have been predefined. These properties of DE have led to an effective entropy measure for biomedical applications [25]. In addition, DE has demonstrated its ability to differentiate between ictal, interictal, and normal EEG signals with a 5 s duration, which is nearly comparable to the performance of whole EEG recordings (above 27 s) [26].

However, DE may ignore quantifying complexity at the multiple temporal scales of a time-series. The MDE has been developed to analyze the multiscale complexity of physiological signals, achieving remarkable performance in describing the complexity of short-term heart rate variability [13,27]. To quantify short epileptic EEG signals, it is essential to reflect the consistent complexity of short-term EEGs and represent underlying complexity over multiple temporal scales [28,29]. The MDE benefits the advantages of DE, i.e., effectiveness for short-term signals. To the best of our knowledge, analysis of epileptic EEG signals using MDE to distinguish between different epileptic states, i.e., ictal, interictal, and normal states, has been lacking.

Here, a family of MDE for differentiating EEG recordings associated with epilepsy is presented. Two approaches are developed: one utilizing coarse-graining to measure DE over multiple time scales and the other using a moving-average to compensate for the stability to the data length. Coarse-graining or moving-average methods allow the proposed MDE to analyze the time series at multiple scales, thereby capturing a more comprehensive picture of the system's dynamics. In addition, different scales can reveal different aspects of the data. For instance, short-term fluctuations might be apparent at finer scales, while long-term trends might only become visible at coarser scales. In this study, the Bonn dataset [30] and the Bern-Barcelona dataset [31], which is the most common EEG analysis dataset for epileptic patients, are used. To exploit the classification performance of short-term EEG recordings, 5 s segments from the beginning, middle, and end intervals of each EEG recording were chosen.

The main contributions of this work are summarized as the following aspects.

1) The proposed MDE methods are presented to serve appropriate features to detect epileptic EEG patterns with short-term EEG signals.
2) The MDE methods are able to compute not only stable entropy values but also consistent entropy values irrespective of the length of EEG signals and the selection of segments of interest from EEG signals, respectively.
3) Using widely used public epileptic EEG datasets, the effectiveness of the proposed MDE methods was validated through statistical analysis and the area under an ROC curve (AUC) analysis, implying their reproducibility and generalization.

The remainder of the paper is structured as follows: Section 2 describes conventional entropy measures, namely SampEn, DE, and MSE, as well as two proposed multiscale evaluations of DE, namely MDE-CG and MDE-MA. In Section 3, the statistical analysis of the experimental results using the Bonn dataset and the Bern-Barcelona dataset is presented. Section 4 presents discussion. Finally, conclusions are presented in Section 5.

2. Materials and methods

2.1. Sample entropy (SampEn)

SampEn is a modified version of ApEn, which utilizes the conditional probability that computes the similarity between two sequences of different lengths m and $m+1$. Here, m denotes the embedding dimension. SamEn differs from ApEn in that SampEn excludes the self-matches in computing entropy values. Specifically, SampEn is computed as follows: First, for a time-series with N sample $\mathbf{x} = \{x_1, x_2, \ldots, x_N\}$, let us construct multidimensional vectors, which are given by

$$\mathbf{X}_i = \{x_i, x_{i+\tau}, \ldots, x_{i+(m-1)\tau}\}, \tag{1}$$

for $1 \le i \le N-(m-1)\tau$. Here, m and τ denote the embedding dimension and time delay, respectively.

Second, the Chebyshev distances $d_{i,j}$ between all possible combinations of vectors $\mathbf{X}_i$ and $\mathbf{X}_j$ are calculated for all $1 \le i, j \le N-(m-1)\tau,\ i \ne j$. Here, the Chebysheve distance is given by

$$d_{i,j} = \max\left(\left|x_{i+k\tau} - x_{j+k\tau}\right|, 0 \le k \le m-1\right) \tag{2}$$

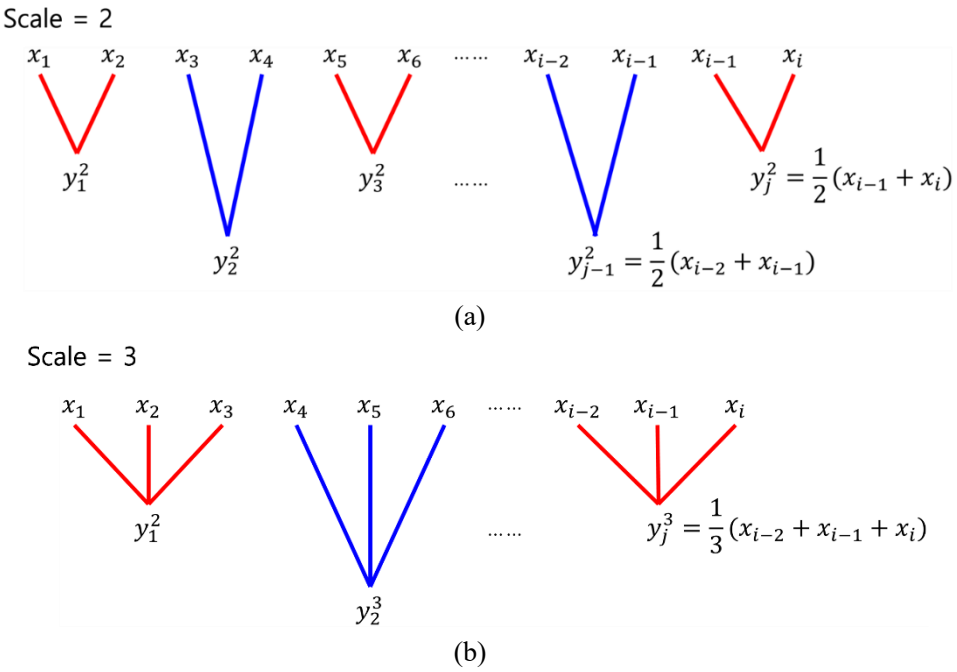

Figure 1. Schematic illustration of the coarse-graining procedure. (a) scale factor s = 2, (b) scale factor s = 3.

Third, let us define $C_i^m(r)$ that represents the probability that a vector $\mathbf{X}_j$ within r of $\mathbf{X}_i$, which is counted if $d_{I,j}$ is less than a threshold parameter r, which is given by

$$C_i^m(r) = \frac{n_i^m(r)}{N-(m-1)\tau}, \tag{3}$$

where r is a threshold parameter, $n_i^m(r)$ is the number of vectors $\mathbf{X}_j$ which meet condition $d_{i,j} \le r$ (that means $\mathbf{X}_j$ is similar to $\mathbf{X}_i$) for all $1 \le i \le N-(m-1)\tau$. Then, this process is repeated when the embedding dimension is $m+1$ to compute $C_i^{m+1}(r)$.

Finally, SampEn is defined by

$$\mathrm{SampEn}(\mathbf{x}, \mathrm{m}, \mathrm{r}, \tau) = -\ln\left[\frac{C^{m+1}}{C^{m}}\right], \tag{4}$$

where $C^{m} = \frac{1}{N-m\tau}\sum_{i=1}^{N-m\tau} C_i^{m}$ and $C^{m+1} = \frac{1}{N-m\tau}\sum_{i=1}^{N-m\tau} C_i^{m+1}$.

It has been known that the higher the SampEn value, the more irregular and complex, thus providing a measure of the complexity of a time-series.

2.2. DE

DE measure quantifies the amount of time-series information based on the probability density estimation of the distance between vectors in the state space [30]. In particular, the DE method consists of the four steps listed below:

First, the multidimensional vector $\mathbf{X}_i$ is reconstructed using Eq (1), which is similar to the SampEn algorithm. Similarly, the inter-vector distances are computed using Eq (2), and the distance matrix is constructed as $D = \{d_{i,j}\}$. Similar to SampEn., it needs to estimate the empirical probability density function (ePDF) of distance matrix D using the histogram approach. Self-matches are ruled out during estimation, so the upper or lower triangular elements of D without diagonal elements can be chosen. The bin size of the histogram is fixed at B, and the probability p_t of each bin is calculated for $1 \le p_t \le B$. Finally, the DE value of $\mathbf{X}_i$ is computed as follows:

$$\mathrm{DE}(\mathbf{x}, m, B, \tau) = -\frac{1}{\log_2 B}\sum_{t=1}^{B} p_t \log_2 p_t \tag{5}$$

2.3. MSE

MSE involves analyzing a time-series at multiple temporal scales. The first step in the MSE analysis is the coarse-graining process. The original time-series is divided into non-overlapping windows of increasing lengths (scales). The data points within a window are averaged at each scale to produce a new time-series that represents that scale. The coarse-graining procedure for generating a new time-series is shown in Figure 1. The coarse-grained time-series y_j^s is computed by Eq (5), in which x_i indicates the original time-series with N samples and s indicates the scale factor as follows:

$$y_j^s = \frac{1}{s}\sum_{i=(j-1)s+1}^{js} x_i, \quad 1 \le j \le \frac{N}{s} \tag{6}$$

where s denotes the scale factor. After coarse-graining, the sample entropy of the resultant time-series y_j^s is calculated at each scale. MSE performs better than conventional single scale-based analysis in most cases. However, MSE provides reliable results when the length of the original time-series is long enough since the coarse-graining process makes the length short [24].

2.4. MDE

Here, two MDE methods that can precisely measure the complexity of short-term EEG by combining DE and two multiscale time-series decomposition methods, namely, coarse-graining and moving-average procedures, are introduced.

Given an N point time-series $\mathbf{x} = \{x_1, x_2, \ldots, x_N\}$, the coarse-graining procedure is applied and the new time-series is developed by Eq (6). Then, DE is used to compute the complexity of the

resultant time-series $\boldsymbol{y}^s = \{y_1^s, y_2^s, \cdots, y_{N/s}^s\}$. Thus, MDE-CG is given by

$$\mathrm{MDE-CG}(\mathbf{x}, m, B, s) = \mathrm{DE}(\boldsymbol{y}^s, m, B, \tau = s). \tag{7}$$

The process of coarse-graining at multiple scales results in a reduction in the length of the original time-series. Consequently, a limitation arises in accurately estimating the complexity of a time-series that is not sufficiently long, leading to potentially erroneous entropy estimates. In order to tackle this issue, a modified multiscale analysis utilizing the moving-averaging technique specifically designed for short-term time-series is employed.

Figure 2 represents the moving-averaging procedure for generating a new time-series. The new time-series y_j^s is reconstructed by overlapping windows with a size of scale factor s from the original time-series $\mathbf{x}$ of N samples. Here, the difference in length between the new time-series and the original one is only $s-1$ samples.

$$y_j^s = \frac{1}{s}\sum_{j=i}^{i+s-1} x_j\,, \quad 1 \le \mathrm{i} \le N - s + 1 \tag{8}$$

where s indicates the scale factor as in Eq (6). If the scale factor $\mathrm{s} = 1$, a moving-averaged time-series $\boldsymbol{y}^{\mathrm{s}} = \{y_1^{\mathrm{s}}, y_2^{\mathrm{s}}, \cdots, y_{\mathrm{N}-2+1}^{\mathrm{s}}\}$ is identical to the original time-series $\boldsymbol{x}$.

Then, DE calculation of the moving-averaged time-series $y_j{}^s$ on each time scale leads to MDE-MA as follows:

$$\mathrm{MDE-MA}(\mathbf{x}, m, B, s) = \mathrm{DE}(\boldsymbol{y}^s, m, B, \tau = s) \tag{9}$$

Note that MDE values for the scale factor $s = 1$ correspond to DE.

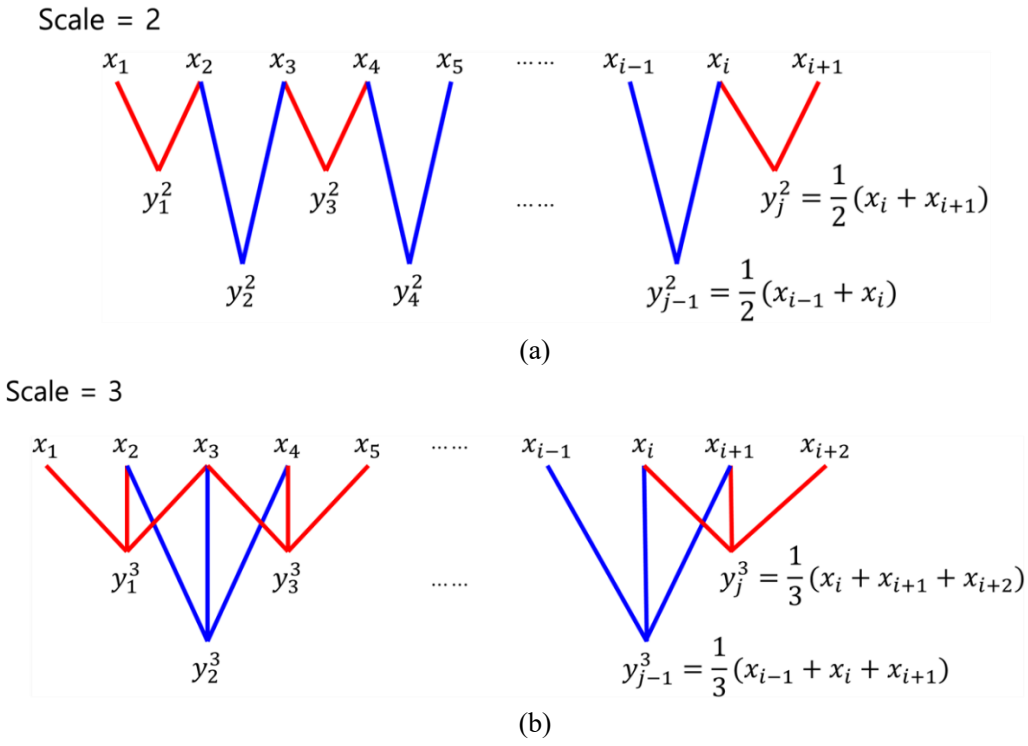

Figure 2. Schematic illustration of the moving-average procedure. (a) scale factor s = 2, (b) scale factor s = 3.

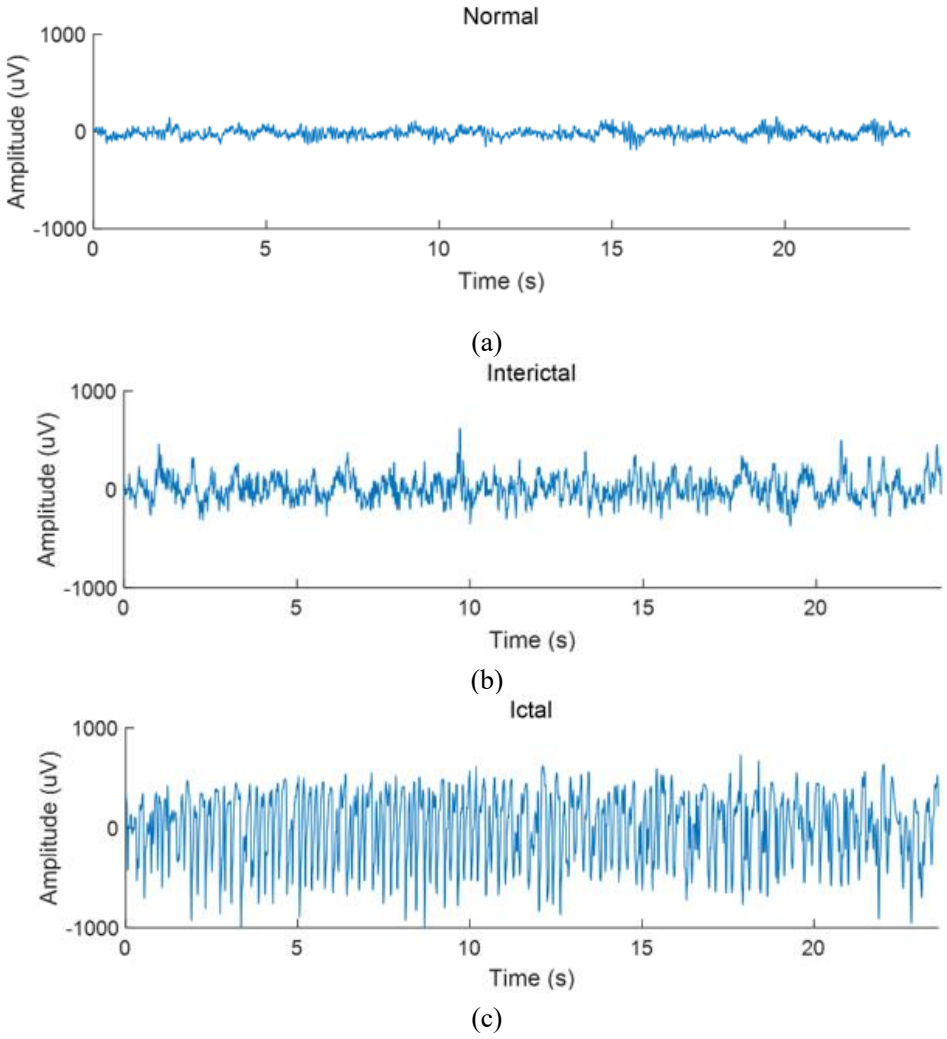

Figure 3. Sample EEG recordings of three states. (a) normal EEG signal (Group Z). (b) interictal (seizure-free) EEG signal (Group N). (c) ictal (seizure) EEG signal (Group S).

2.5. EEG data

In this study, two datasets are utilized. First, the Bonn dataset is used, which is one of the most widely used public datasets in the field of epileptic seizure detection [30]. The dataset consists of 500 individual single-channel EEG recordings sampled at a frequency of 173.61 Hz. Each recording has a duration of 23.6 seconds. The recordings are classified into five distinct categories, namely classes Z, O, N, F, and S, with each group including a total of 100 recordings. Sets Z and O were measured from five healthy volunteers while their eyes were open and closed in an awake state, respectively. Sets N, F, and S were measured from patients with epilepsy, all of whom had achieved complete seizure control after the resection of one of the hippocampal formations. Set N was measured from the hippocampal formation of the opposite hemisphere of the brain and set F was measured within the epileptogenic zone during seizure-free intervals. set E was recorded during seizures (i.e., in the ictal state). To distinguish normal, interictal, and ictal states, we categorized sets Z and O as normal groups, sets N and F as interictal groups, and set S as an ictal group. Figure 3(a)−(c) show the actual sample EEG recordings for normal, interictal and ictal periods, respectively.

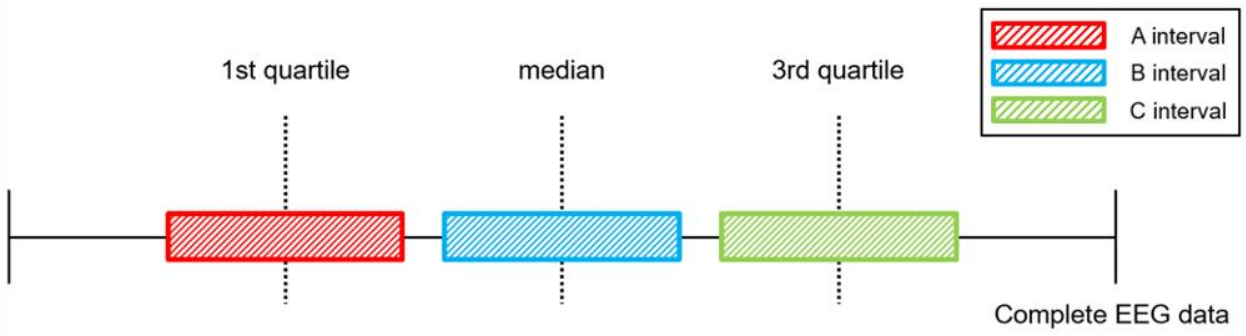

Figure 4. Three intervals with 5 seconds duration segmented from a complete EEG recording. Data from A, B, and C intervals are set around the first quartile, median, and third quartile, respectively.

To detect seizures in short-length EEG, three segments of EEG with a length of 868 sampling points (5 seconds) from the original EEG data contained in each set are utilized, as shown in Figure 4. The window length was set to 5 seconds since EEG recordings of 5 seconds effectively reflect the epileptic states [26]. Instead of segmenting complete EEG into short-length EEG data blocks randomly, three intervals are selected: (A) the segment was extracted from the initial phase of the recording, with its midpoint positioned at the first quartile; (B) the segment was extracted from the middle phase, with its midpoint aligned at the median; (C) the segment was extracted from the later phase of the recording, with its midpoint aligned at the third quartile.

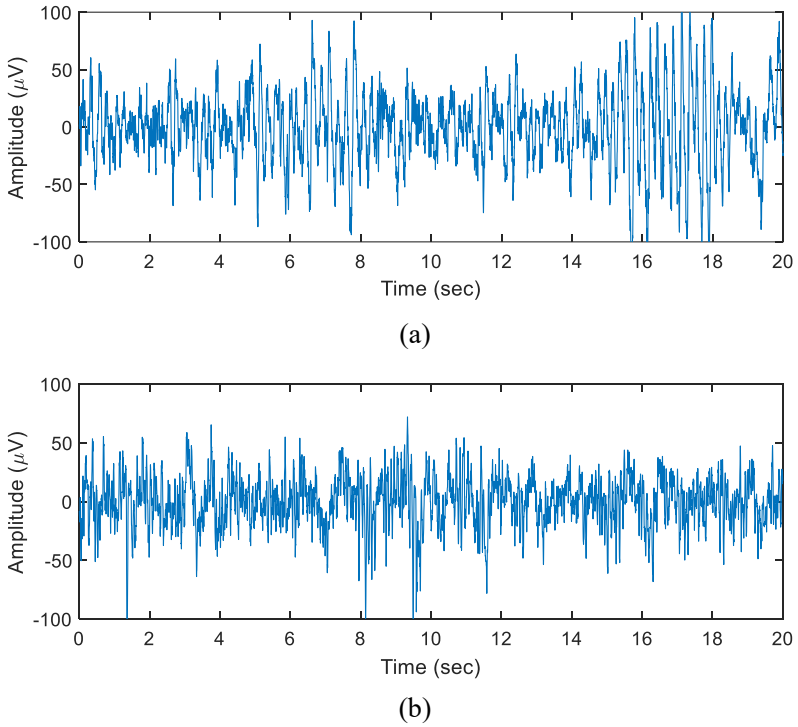

Figure 5. Sample EEG recordings of two states. (a) focal EEG signal. (b) non-focal EEG signal.

Secondly, the Bern-Barcelona dataset was employed. The EEG signals of five individuals with long-standing pharmacoresistant temporal lobe epilepsy who are candidates for epilepsy surgery are included in this dataset [31]. The EEG signals of five individuals with chronic pharmacoresistant temporal lobe epilepsy who are candidates for epilepsy surgery are included in this dataset and sampled at a frequency of 512 Hz. The focus channel, which identified initial ictal EEG signal alterations and was evaluated visually by a minimum of two clinical specialists. Non-focal channels refer to the remaining channels. Figure 5(a),(b) depict the focal and non-focal EEG recordings, respectively.

3. Experimental results

3.1. Results with entropy values

Figure 6 depicts the entropy values of MSE, MDE-CG, and MDE-MA utilizing three segments of EEGs, namely the A, B, and C intervals in Figure 4, from complete EEGs of normal, interictal, and ictal groups. The entropy values are computed on a scale factor $1 \leq s \leq 20$. The parameters of the MSE were set to $r = 0.15\sigma$, $m = 2$, and $\tau = 8$, where σ denotes the standard deviation of a EEG signal [16,32]. For the proposed MDE-CG and MDE-MA, the parameters $m = 2$, $\tau = 8$, and $B = 64$ were used.

Figures 6(a)−(c) exhibit the MSE, MDE-CG, and MDE-MA results for the A interval, respectively. In Figure 6(a), the MSE values at the scale factors are not more than 7, and they show different levels of entropy values across normal, interictal, and ictal EEGs. However, for larger scale factors ($s \geq 7$), the MSE values are not evaluated due to the dependency of MSE on the length of coarse-grained time-series. In addition, the MSE values of normal EEGs are highest among the three groups, while those of ictal EEGs are lowest at the range of the scale factors less than 6.

In Figure 6(b), the MDE-CG values of three different epileptic states are distinguishable: the entropy values of the ictal EEGs are higher than those of other EEGs, and normal EEGs have the lowest values for all scale factors. Compared to Figure 6(b), the MDE-MA values of the three groups are more differentiable for all scale factors, as shown in Figure 6(c). In Figure 6(b),(c), the three groups using the proposed MDE-CG and MDE-MA are distinguishable, especially between normal and epileptic EEGs in that the MDE-CG and MDE-MA values of normal EEGs are lower than interictal and ictal EEGs, compared to the MSE. In addition, the MDE-CG and MDE-MA values of interictal EEGs and normal EEGs are lower than those of ictal EEGs for all scale factors. Notably, the MDE-MA values for all scale factors fluctuate less than the MDE-CG. The MSE values are not evaluated due to the dependency of MSE on the length of the coarse-grained time-series. In addition, the MSE values of normal EEGs are highest among the three groups, while those of ictal EEGs are lowest at the range of the scale factors less than 6.

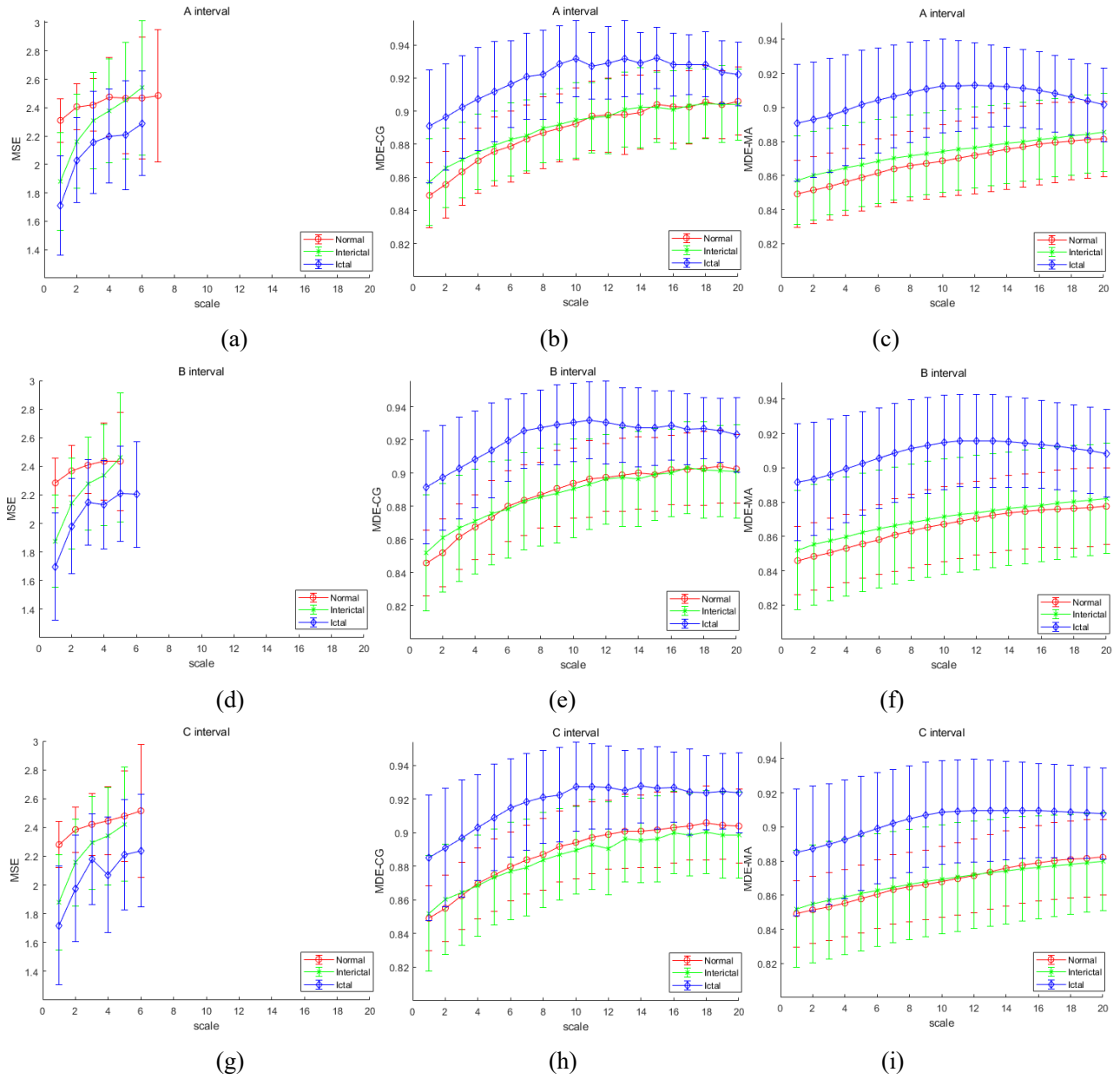

Figure 6. The results of MSE, MDE-CG, and MDE-MA analyzing EEGs contained in 3 epileptic state groups at 3 intervals. (a) MSE result for A interval, (b) MDE-CG result for A interval, (c) MDE-MA result for A interval, (d) MSE result for B interval, (e) MDE-CG result for B interval, (f) MDE-MA result for B interval, (g) MSE result for C interval, (h) MDE-CG result for C interval, (i) MDE-MA result for C interval. The values on each scale are expressed as mean $\pm$ standard deviation.

Compared with the previous works, which use SampEn and DE, the MDE-CG and MDE-MA provide quantification tools over multiple time scales in that conventional entropy can quantify complexity at a single scale ($s = 1$). Furthermore, the computation of MDE-CG and MDE-MA over multiple time scales results in more capable differentiation between epileptic EEGs: the entropy values not only become higher in the order of ictal, interictal, and normal EEGs but also the difference between entropy values of distinct epileptic states are more significant. This implies that MDE-CG and MDE-MA might play a critical role in quantifying the complexity of distinct epileptic EEGs that can be used

between different epileptic states of EEGs. This result correlates with previous findings in [26] that they have the highest entropy values in the order of ictal, interictal, and normal EEGs. These results correspond to the results of MDEs with a scale factor of 1.

Figure 6(d)−(f) show the MSE, MDE-CG, and MDE-MA results for the B interval, respectively. As shown in Figure 5(d), the MSE values at less than scale factor 6 are distinguishable between the three groups. However, as shown in the figure, the MSE values are undefined across larger scale factors, which is similar to the results of Figure 6(a). The entropy values of MSE for the three groups are presented in the following order: normal, interictal, and ictal EEGs, which is also similar to the results of Figure 6(a).

In Figure 6(e),(f), the difference in entropy values of MDE-CG and MDE-MA between the three groups widen compared to MSE, similar to Figures 6(b),(c). Specifically, the MDE-CG and MDE-MA values of ictal EEGs are highest for all scale factors, followed by the interictal and normal EEGs. The MDE-CG values of interictal EEGs are higher than those of normal EEGs at small scale factors ($s \leq 5$), while the MDE-CG values of the two groups are similar at larger scale factors, as shown in Figure 6(e). Compared with the results of MDE-CG shown in Figure 6(e), the MDE-MA values of interictal and normal EEGs are more differentiable over most scale factors, as shown in Figure 6(f). It suggests that MDE-MA is more capable of quantifying the underlying complexities of epileptic and normal EEGs than MDE-CG due to the use of moving average process.

Figure 6(g)−(i) show the MSE, MDE-CG, and MDE-MA results from all the EEG recordings for the C interval. The results of MSE, MDE-CG, and MDE-MA for the C interval of three epileptic groups show similar quantification compared to the results of intervals A and B.

In Figure 6, we found that MSE, MDE-CG, and MDE-MA have comparable quantification of complexity with different protocols, implying those measures possess consistency for the selection of epileptic EEGs.

3.2. Statistical analysis

In this section, statistical analysis was performed to verify the performance of MSE and two proposed MDE methods. The Mann-Whitney U test was performed to validate the statistical significance of the distinction using the above entropy methods using EEGs from three different physiological states. The Mann-Whitney U test was utilized to verify the statistical differences between the entropy values of the three EEGs. Each statistical analysis was carried out by comparing different physiological states, namely, normal vs. interictal, normal vs. ictal, and interictal vs. ictal. The significance level for the decision of hypothesis testing is set to 0.001, so if the p-value is less than 0.001, statistical significance is accepted and indicated as shaded in Table. Tables 1−3 show the analysis results of MSE, MDE-CG, and MDE-MA, respectively.

Table 1 shows the statistical analysis results for the MSE results for three cases of comparisons for different short-term intervals from entire EEG recordings. On a limited number of time scales, it is able to distinguish between normal and interictal EEGs, regardless of the selection of intervals.

Table 1. The results of the Mann—Whitney U test for MSE values.

Scale factor	[a]p-value								
	A interval			B interval			C interval		
	N / Inter	N / Ictal	Inter / Ictal	N / Inter	N / Ictal	Inter / Ictal	N / Inter	N / Ictal	Inter / Ictal
1	1.98×10^{-34}	1.07×10^{-36}	1.69×10^{-5}	2.33×10^{-41}	9.57×10^{-37}	1.21×10^{-4}	5.13×10^{-38}	2.65×10^{-33}	0.003
2	2.90×10^{-19}	8.96×10^{-27}	9.25×10^{-6}	5.25×10^{-18}	1.24×10^{-25}	8.17×10^{-6}	9.12×10^{-19}	1.64×10^{-23}	5.81×10^{-5}
3	0.003	3.66×10^{-13}	5.32×10^{-6}	1.51×10^{-4}	9.56×10^{-14}	1.19×10^{-5}	4.32×10^{-5}	1.14×10^{-10}	0.001
4	0.011	2.84×10^{-12}	2.83×10^{-6}	0.023	4.78×10^{-16}	2.05×10^{-9}	5.03×10^{-4}	7.10×10^{-16}	1.37×10^{-7}
5	0.650	3.05×10^{-8}	1.16×10^{-7}	0.219	5.54×10^{-7}	8.12×10^{-8}	0.233	3.08×10^{-10}	7.23×10^{-7}
6	0.089	0.002	0.94×10^{-6}	N/A	N/A	N/A	N/A	8.51×10^{-7}	N/A
7~20	[b]N/A	N/A	N/A	N/A	N/A	N/A	N/A	N/A	N/A

The shadow denotes that the two groups are significantly different ($p < 0.001$). N/A denotes "Not Available". "N" indicates the normal group, 'Inter' indicates the interictal group, and "Ictal" indicates the ictal group.

Table 2. The results of the Mann—Whitney U test for MDE-CG values.

Scale factor	[a]p-value								
	A interval			B interval			C interval		
	N / Inter	N / Ictal	Inter / Ictal	N / Inter	N / Ictal	Inter / Ictal	N / Inter	N / Ictal	Inter / Ictal
1	1.22×10^{-4}	2.98×10^{-24}	8.13×10^{-17}	8.06×10^{-6}	1.20×10^{-27}	2.93×10^{-20}	1.01×10^{-4}	5.77×10^{-18}	3.58×10^{-12}
2	6.50×10^{-6}	1.12×10^{-24}	3.16×10^{-16}	6.01×10^{-8}	3.17×10^{-29}	9.63×10^{-20}	2.10×10^{-4}	9.91×10^{-19}	8.42×10^{-12}
3	0.002	5.55×10^{-26}	4.13×10^{-19}	2.95×10^{-4}	5.03×10^{-28}	1.47×10^{-20}	0.086	1.41×10^{-17}	5.55×10^{-13}
4	0.011	1.24×10^{-22}	2.63×10^{-17}	0.005	3.34×10^{-27}	9.00×10^{-21}	0.944	2.36×10^{-18}	3.16×10^{-16}
5	0.127	3.24×10^{-21}	2.00×10^{-18}	0.036	2.57×10^{-26}	3.05×10^{-22}	0.990	1.46×10^{-18}	7.39×10^{-17}
6	0.034	3.52×10^{-25}	4.42×10^{-21}	0.593	8.42×10^{-28}	7.63×10^{-27}	0.774	2.19×10^{-21}	5.22×10^{-20}
7	0.127	4.05×10^{-26}	4.73×10^{-24}	0.357	1.05×10^{-31}	2.33×10^{-30}	0.118	2.91×10^{-21}	3.52×10^{-21}
8	0.253	3.36×10^{-22}	2.74×10^{-20}	0.432	7.40×10^{-31}	7.44×10^{-28}	0.354	4.48×10^{-21}	8.64×10^{-21}
9	0.207	1.28×10^{-28}	4.30×10^{-26}	0.707	1.00×10^{-26}	2.46×10^{-26}	0.047	3.56×10^{-18}	4.02×10^{-19}
10	0.283	1.40×10^{-29}	1.85×10^{-26}	0.734	2.18×10^{-26}	5.47×10^{-25}	0.080	1.26×10^{-20}	2.66×10^{-22}
11	0.461	2.16×10^{-24}	3.73×10^{-25}	0.543	5.15×10^{-24}	2.19×10^{-25}	0.240	2.05×10^{-18}	1.14×10^{-19}
12	0.873	1.22×10^{-21}	8.47×10^{-23}	0.912	1.40×10^{-22}	2.71×10^{-20}	0.004	3.38×10^{-18}	1.56×10^{-21}
13	0.158	1.38×10^{-22}	3.43×10^{-20}	0.751	2.11×10^{-20}	5.70×10^{-18}	0.091	1.01×10^{-14}	1.02×10^{-16}
14	0.121	2.16×10^{-22}	2.61×10^{-18}	0.463	1.22×10^{-17}	2.99×10^{-18}	0.049	3.06×10^{-18}	3.07×10^{-21}
15	0.552	3.01×10^{-22}	9.69×10^{-24}	0.505	9.50×10^{-20}	4.75×10^{-17}	0.060	1.65×10^{-14}	9.32×10^{-18}
16	0.592	1.27×10^{-17}	1.17×10^{-19}	0.633	2.97×10^{-20}	1.36×10^{-18}	0.294	1.21×10^{-15}	6.80×10^{-17}
17	0.757	3.21×10^{-20}	8.30×10^{-19}	0.353	2.95×10^{-16}	8.17×10^{-12}	0.048	3.78×10^{-11}	1.03×10^{-13}
18	0.325	5.60×10^{-16}	5.10×10^{-18}	0.891	1.36×10^{-17}	9.90×10^{-15}	0.037	9.54×10^{-10}	1.77×10^{-13}
19	0.812	1.09×10^{-13}	8.67×10^{-12}	0.683	2.19×10^{-14}	1.82×10^{-14}	0.021	2.08×10^{-13}	1.46×10^{-15}
20	0.339	7.18×10^{-10}	1.44×10^{-11}	0.758	5.84×10^{-12}	$1/06\times10^{-10}$	0.078	1.31×10^{-10}	3.78×10^{-13}

The shadow denotes that the two groups are significantly different ($p < 0.001$).

Table 3. The results of the Mann—Whitney U test for MDE-MA values.

Scale factor	[a]p-value								
	A interval			B interval			C interval		
	N / Inter	N / Ictal	Inter / Ictal	N / Inter	N / Ictal	Inter / Ictal	N / Inter	N / Ictal	Inter / Ictal
1	1.22×10^{-4}	2.98×10^{-24}	8.13×10^{-17}	8.06×10^{-6}	1.20×10^{-27}	2.93×10^{-20}	1.01×10^{-4}	5.77×10^{-18}	3.58×10^{-12}
2	6.50×10^{-6}	1.12×10^{-24}	3.16×10^{-16}	6.01×10^{-8}	3.17×10^{-29}	9.63×10^{-20}	2.10×10^{-4}	9.91×10^{-19}	8.42×10^{-12}
3	0.002	5.55×10^{-26}	4.13×10^{-19}	2.95×10^{-4}	5.03×10^{-28}	1.47×10^{-20}	0.086	1.41×10^{-17}	5.55×10^{-13}
4	0.011	1.24×10^{-22}	2.63×10^{-17}	0.005	3.34×10^{-27}	9.00×10^{-21}	0.944	2.36×10^{-18}	3.16×10^{-16}
5	0.127	3.24×10^{-21}	2.00×10^{-18}	0.036	2.57×10^{-26}	3.05×10^{-22}	0.990	1.46×10^{-18}	7.39×10^{-17}
6	0.034	3.52×10^{-25}	4.42×10^{-21}	0.593	8.42×10^{-28}	7.63×10^{-27}	0.774	2.19×10^{-21}	5.22×10^{-20}
7	0.127	4.05×10^{-26}	4.73×10^{-24}	0.357	1.05×10^{-31}	2.33×10^{-30}	0.118	2.91×10^{-21}	3.52×10^{-21}
8	0.253	3.36×10^{-22}	2.74×10^{-20}	0.432	7.40×10^{-31}	7.44×10^{-28}	0.354	4.48×10^{-21}	8.64×10^{-21}
9	0.207	1.28×10^{-28}	4.30×10^{-26}	0.707	1.00×10^{-26}	2.46×10^{-26}	0.047	3.56×10^{-18}	4.02×10^{-19}
10	0.283	1.40×10^{-29}	1.85×10^{-26}	0.734	2.18×10^{-26}	5.47×10^{-25}	0.080	1.26×10^{-20}	2.66×10^{-22}
11	0.461	2.16×10^{-24}	3.73×10^{-25}	0.543	5.15×10^{-24}	2.19×10^{-25}	0.240	2.05×10^{-18}	1.14×10^{-19}
12	0.873	1.22×10^{-21}	8.47×10^{-23}	0.912	1.40×10^{-22}	2.71×10^{-20}	0.004	3.38×10^{-18}	1.56×10^{-21}
13	0.158	1.38×10^{-22}	3.43×10^{-20}	0.751	2.11×10^{-20}	5.70×10^{-18}	0.091	1.01×10^{-14}	1.02×10^{-16}
14	0.121	2.16×10^{-22}	2.61×10^{-18}	0.463	1.22×10^{-17}	2.99×10^{-18}	0.049	3.06×10^{-18}	3.07×10^{-21}
15	0.552	3.01×10^{-22}	9.69×10^{-24}	0.505	9.50×10^{-20}	4.75×10^{-17}	0.060	1.65×10^{-14}	9.32×10^{-18}
16	0.592	1.27×10^{-17}	1.71×10^{-19}	0.633	2.97×10^{-20}	1.46×10^{-18}	0.294	1.21×10^{-15}	6.80×10^{-17}
17	0.757	3.21×10^{-20}	8.30×10^{-19}	0.353	2.95×10^{-16}	8.17×10^{-12}	0.048	3.78×10^{-11}	1.03×10^{-13}
18	0.325	5.60×10^{-16}	5.10×10^{-18}	0.891	1.36×10^{-17}	9.90×10^{-15}	0.037	9.54×10^{-10}	1.77×10^{-13}
19	0.812	1.09×10^{-13}	8.67×10^{-12}	0.683	2.19×10^{-14}	1.82×10^{-14}	0.021	2.08×10^{-13}	1.46×10^{-15}
20	0.339	7.18×10^{-10}	1.44×10^{-11}	0.758	5.84×10^{-12}	1.06×10^{-10}	0.078	1.31×10^{-10}	3.78×10^{-13}

The shadow denotes that the two groups are significantly different $(p < 0.001)$.

In addition, the distinction between normal and ictal, and interictal and ictal EEGs is statistically significant below a scale factor of 6. For larger time scales, statistical analysis is unavailable due to the existence of a number of undefined entropy values. The statistical results are similar for the different intervals.

In Table 2, the statistical analysis results using MDE-CG are shown. The p-values of comparison between normal and ictal EEGs and interictal and ictal EEGs for all scale factors are less than 0.001 regardless of the intervals. This implies that the differentiation between normal and ictal EEGs, and interictal and ictal EEGs is statistically significant.

On the other hand, the normal and interictal EEGs are differentiable on small scale factors (less than 2 for A and C intervals, and less than 3 for B intervals, respectively). Compared to the results of MSE analysis, the proposed MDE-CG has improved performance in distinguishing between normal and epileptic EEGs, especially between normal and interictal EEGs, and interictal and ictal EEGs.

Table 3 exhibits the statistical analysis results of MDE-MA. As can be seen, the use of MDE-MA leads to the ability to distinguish between normal and epileptic EEGs, especially between normal and interictal EEGs, and interictal and ictal EEGs. For the comparison between normal and interictal EEGs, MDE-MA is better capable of differentiating two distinct EEGs for a wider range of scale factors compared to MSE and MDE-CG, implying the superiority of MDE-MA.

3.3. Evaluation of classification performance

Here, we evaluated the classification performance of the MSE, MDE-CG, and MDE-MA between three distinct EEGs, i.e., normal, interictal and ictal EEGs using receiver operating characteristic (ROC) curve analysis. The classification performance for each entropy method was evaluated as AUC.

Figure 7 depicts the AUC results of the MSE, MDE-CG and MDE-MA methods for classification between three different states of EEGs by pairwise comparison. As in previous experiments, three distinct intervals from a whole EEG recording were chosen and used for classification.

Figures 7(a)−(c) show the AUC results of MSE, MDE-CG, and MDE-MA for the A interval, respectively. Comparing with the classifications between normal and ictal EEGs, and interictal and ictal EEGs, the classification between normal and interictal is the worst performing. In Figure 7(a), MSE has higher AUC values at scale factors 1 and 2 than the two MDE methods. In Figure 7(b), regarding the classification between normal and ictal EEGs, the MDE-CG and MDE-MA methods show better classification performance except for the scale factor of 1. Moreover, the classification performance of MDE-MA is slightly better than that of MDE-CG. Figure 7(c) shows that MDE-CG and MDE-MA perform better than MSE in differentiating interictal and ictal EEGs.

Figures 7(d)−(f) exhibit the AUC results of three entropy measures for the B interval. The AUC results of MSE, MDE-CG and MDE-MA shown in Figures 7(d)−(f) are similar to those of the A interval, shown in Figures 7(a)−(c). Figures 7(g)−(i) show that the AUC results of the C interval are comparable to those of the other two intervals. These imply that the discrimination of distinct epileptic EEGs is less dependent on selecting short-term EEGs from a whole EEG recording.

The AUC results in Figure 7 suggest that MSE values at restricted small scales work better for differentiating interictal EEGs from normal EEGs. For other classifications, namely normal and ictal EEG, and interictal and ictal EEGs, MDE-MA, MDE-CG, and MSE, in that order, perform well.

Through experiments, MDE-CG and MDE-MA have proven their effectiveness for differentiating epileptic states using short-term EEG recording compared to conventional DE. The use of MDE for multiple scales leads to increased features that quantify the complexities of EEGs. It might help in the detection of interictal and ictal EEGs more accurately than conventional complexity measures.

ROC curve analysis was performed for the binary classification between the focal and non-focal EEGs using the Bern-Barcelona dataset, followed by AUC evaluation for classification performance.

Figure 8 shows the AUC results of the MSE, MDE-CG, and MDE-MA for classification between focal and non-focal EEGs. As can be seen, MSE has higher AUC values at the scale factor of 1 than its competitors. However, for the other scale factors, MDE-MA performs the highest AUC values followed by MDE-CG and MSE. Moreover, MSE fails to classify the focal and non-focal EEGs. Figure 8's AUC values suggest that MDE-MA may be a superior quantification tool for both focal and non-focal EEGs. MDE-CG exhibits comparable performance to MDE-MA, whereas MSE demonstrates the lowest performance among the three multiscale-based entropy methods.

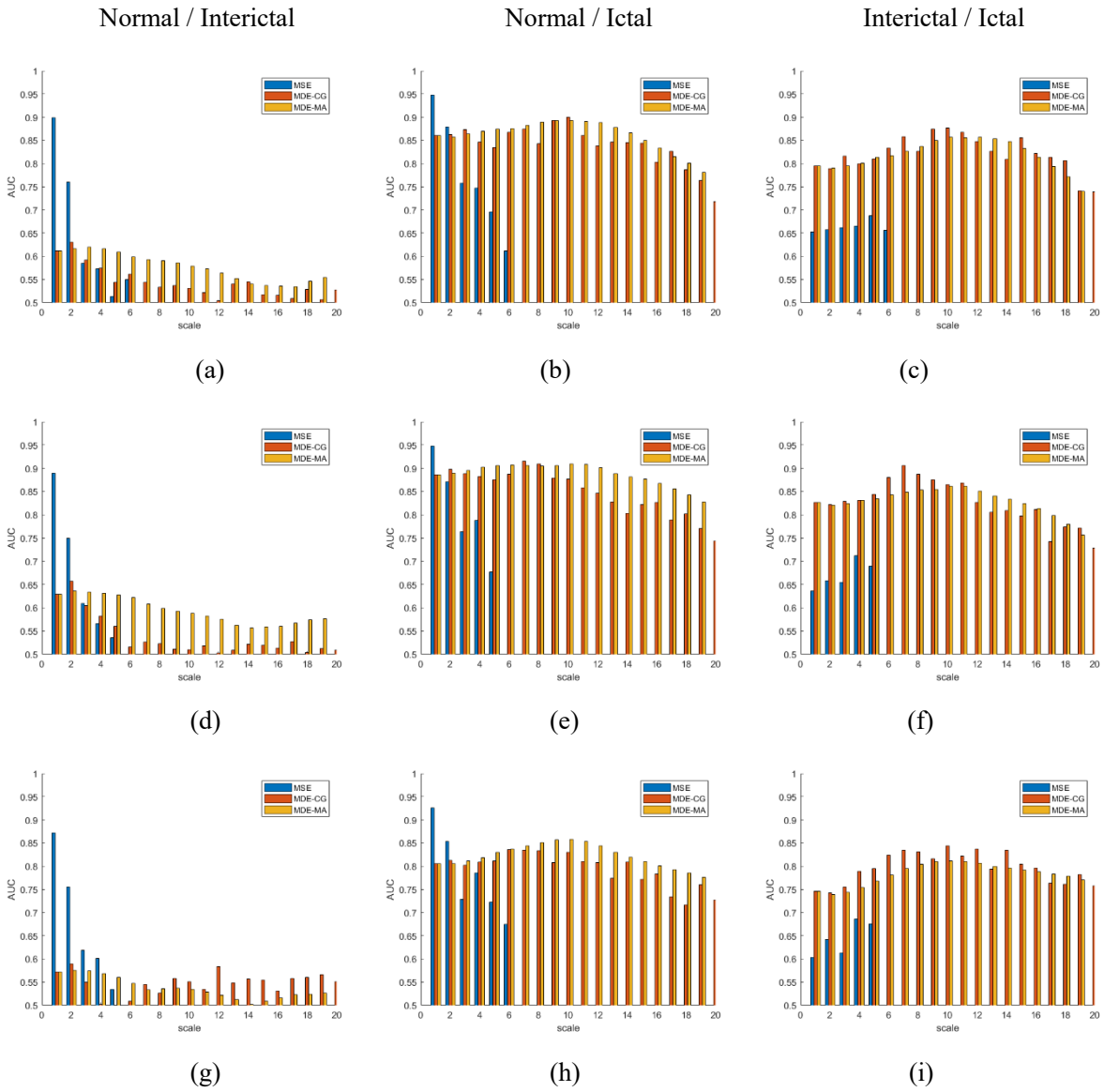

Figure 7. Area under the ROC curve (AUC) results of MSE, MDE-CG, and MDE-MA values for all pairs of EEG data at 3 intervals. (a) performances to distinguish between normal and interictal groups at interval A, (b) performances to distinguish between normal and ictal groups at interval A, (c) performances to distinguish between interictal and ictal groups at interval A, (d) performances to distinguish between normal and interictal groups at interval B, (e) performances to distinguish between normal and ictal groups at interval B, (f) performances to distinguish between interictal and ictal groups at interval B, (g) performances to distinguish between normal and interictal groups at interval C, (h) performances to distinguish between normal and ictal groups at interval C, (i) performances to distinguish between interictal and ictal groups at interval C.

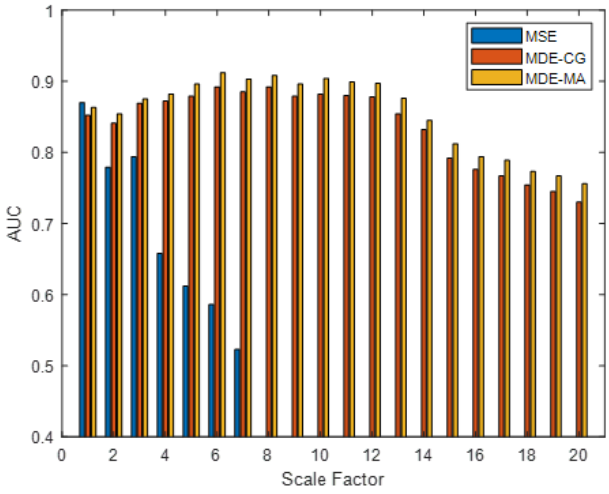

Figure 8. AUC results of MSE, MDE-CG, and MDE-MA values for classification of focal and non-focal EEGs.

4. Discussion

This work presents two versions of MDE utilizing a coarse-graining and moving average process with application to the analysis of the epileptic EEG recordings with the aim of detecting epileptic EEG recordings rapidly.

As a means of representing the complexity of EEG signals, a variety of entropy measures have assumed prominence in recent years. While the relationship between entropy and complexity is still a matter of debate, entropy estimation of neurophysiological signals can serve as a partial representation of the complexity of the neural systems that lie beneath.

MSE, the well-known entropy measure, offers a resolution to the problem of complexity-induced inconsistency. On account of its capabilities, MSE has been implemented in a vast array of settings, including biomedical environments. Unlike other applications, the utilization of EEG recordings requires specific considerations. Rapidly and precisely determining the significance of a signal quantitatively is an indispensable skill.

Recent progress in developing capable entropy measures to detect epileptic patterns from short-term EEG recordings has been made [9,33]. Along this line of thought, a better entropy method, which reflects the complexity of epileptic EEG signals by addressing the inconsistency between complexity and entropy, is lacking. While a timely and robust estimation of epileptic EEG signals is of great importance since the stable and consistent computation of entropy values results in real-time detection of epileptic EEG signals, it encounters obstacles.

This work's exploration into the complexity of short-term EEG signals has yielded promising results that stand to enhance our understanding and management of epileptic seizures. The introduction of MDE-CG and MDE-MA methods marks a significant advancement in quantifying the complexity of EEG signals, especially for short-term EEG recordings comparing the results obtained with widely used MSE. In addition, the performance of the proposed MDE methods was consistent regardless of the choice of intervals in the EEG signal. In summary, the MDE-based epileptic seizure detection methods are better able to capture not only stable features using short EEG signals but also consistent

features regardless of the choice of intervals in the EEG signal, implying its practicality. This brevity is crucial for real-time seizure detection applications, where speed and accuracy are imperative for patient safety and treatment efficacy. The proposed work has limitations in analyzing multichannel epileptic EEG recordings.

It is worth noting that current work has limitations in dealing with datasets. First, since the Bonn dataset is mixed with scalp and intracranial EEG recordings, it needs to be validated using other epileptic EEG datasets. Second, subject-independent experiments are needed to validate the practical effectiveness.

Recently, from other applications such as fault diagnosis of bearing, capable and effective multiscale-based entropy measures have been developed, showing their superiority. Adopting these methods can improve the performance of detecting abnormalities in signals, including epileptic EEGs.

However, it is facing challenges due to the lack of an epileptic EEG database. To enhance the generalized ability to detect epilepsy seizures, it is advisable to utilize modern and sophisticated artificial intelligence (AI) techniques, particularly incorporating multimodal and self-supervised learning [34,35]. In addition, applying various capable deep-learning methods for detecting epilepsy seizures would enhance the effectiveness of this line of work [36–41].

The work lays the stage for future research on applying these approaches to various datasets and real-world situations. Validation across diverse patient populations and seizure types will be essential for universal adoption.

5. Conclusions

This work has presented effective quantification methods for distinguishing several types of epileptic EEG signals, including ictal, interictal, and normal EEGs, as well as focal and non-focal seizures, through the multiscale entropy analysis of short-term recordings. A multiscale-based DE quantification has been developed for timely and reproducible quantification of the complexity of EEGs over multiple temporal scales. The resultant MDE-CG and MDE-MA incorporate DE computation and the coarse-graining and moving-average procedures, respectively.

Computing MDEs for a distinct selection of short-term segments of EEGs shows that the MDEs are stable and consistent with short-term EEGs. Experimental results using two public epileptic EEG datasets indicate that the proposed MDEs outperform the conventional MSE in the following aspects.

1) The MDEs lead to remarkably more statistically significant comparison cases (p-values < 0.001) than MSE, especially for discrimination between ictal and normal EEGs, and ictal and interictal EEGs.
2) AUC values of the MDEs over multiple scales are much higher than those of MSE for all two datasets.

This capability of the proposed MDEs implies that the MDE-CG and MDE-MA may play a role as prospective tools for practical epileptic seizure detection scenarios in cases where timely and precise decisions for epileptic patients are imperative. In addition, to better detect epileptic patterns in EEGs, a multivariate version of multiscale entropy would be preferred since a multivariate multiscale dynamic indicator can reflect the spatial dynamic complexity of the recordings. Future works include increasing generalization for detecting epileptic EEG signals by augmenting epileptic EEG datasets or applying multimodal and self-supervised learning approaches.

Use of AI tools declaration

The authors declare that they have not used Artificial Intelligence (AI) tools in the creation of this article.

Acknowledgments

This research was partly supported by the MSIT(Ministry of Science and ICT), Korea, under the ITRC(Information Technology Research Center) support program(IITP-2024-RS-2022-00156225) supervised by the IITP(Institute for Information & Communications Technology Planning & Evaluation) and by the Excellent researcher support project of Kwangwoon University in 2022.

Conflict of interest

The authors declare that there is no conflict of interest.

References

1. A. K. Ngugi, C. Bottomley, I. Kleinschmidt, J. W. Sander, C. R. Newton, Estimation of the burden of active and life-time epilepsy: A meta-analytic approach, *Epilepsia*, **51** (2010), 883–890. https://doi.org/10.1111/j.1528-1167.2009.02481.x
2. W. A. Hauser, E. Beghi, First seizure definitions and worldwide incidence and mortality, *Epilepsia*, **49** (2008), 8–12.
3. R. S. Fisher, C. Acevedo, A. Arzimanoglou, A. Bogacz, J. H. Cross, C. E. Elger, et al., ILAE official report: A practical clinical definition of epilepsy, *Epilepsia*, **55** (2014), 475–482. https://doi.org/10.1111/epi.12550
4. O. Devinsky, T. Spruill, D. Thurman, D. Friedman, Recognizing and preventing epilepsy-related mortality: A call for action, *Neurology*, **86** (2016), 779–786.
5. H. O. Lüders, I. Najm, D. Nair, P. Widdess-Walsh, W. Bingman, The epileptogenic zone: general principles, *Epileptic Disord.*, **8** (2006), 1–2. https://doi.org/10.1684/j.1950-6945.2006.tb00152.x
6. Y. Paul, Various epileptic seizure detection techniques using biomedical signals: A review, *Brain Inf.*, **5** (2018). https://doi.org/10.1186/s40708-018-0084-z
7. S. Noachtar, J. Rémi, The role of EEG in epilepsy: A critical review, *Epilepsy Behav*., **15** (2009), 22–33. https://doi.org/10.1016/j.yebeh.2009.02.035
8. U. Seneviratne, M. Cook, W. D'Souza, Brainwaves beyond diagnosis: Wider applications of electroencephalography in idiopathic generalized epilepsy, *Epilepsia*, **63** (2022), 22–41. https://doi.org/10.1111/epi.17119
9. R. Cherian, E. G. Kanaga, Theoretical and methodological analysis of EEG based seizure detection and prediction: An exhaustive review, *J. Neurosci. Methods*, **369** (2022), 109483. https://doi.org/10.1016/j.jneumeth.2022.109483
10. S. J. J. Jui, R. C. Deo, P. D. Barua, A. Devi, J. Soar, U. R. Acharya, Application of entropy for automated detection of neurological disorders with electroencephalogram signals: A review of the last decade (2012–2022), *IEEE Access*, **11** (2023), 71905–71924. https://doi.org/10.1109/ACCESS.2023.3294473

11. A. Ulate-Campos, F. Coughlin, M. Gaínza-Lein, I. S. Fernández, P. L. Pearl, T. Loddenkemper, Automated seizure detection systems and their effectiveness for each type of seizure, *Seizure*, **40** (2016), 88–101. https://doi.org/10.1016/j.seizure.2016.06.008
12. A. Shoeibi, N. Ghassemi, R. Alizadehsani, M. Rouhani, H. Hosseini-Nejad, A. Khosravi, et al., A comprehensive comparison of handcrafted features and convolutional autoencoders for epileptic seizures detection in EEG signals, *Expert Syst. Appl.*, 163 (2021), 113788. https://doi.org/10.1109/ACCESS.2023.3294473
13. D. Y. Lee, Y. S. Choi, Multiscale distribution entropy analysis of short-term heart rate variability, *Entropy*, **20** (2018), 952. https://doi.org/10.3390/e20120952
14. V. Srinivasan, C. Eswaran, N. Sriraam, Approximate entropy-based epileptic EEG detection using artificial neural networks, *IEEE Trans. Inf. Technol. Biomed.*, **11** (2007), 288–295. https://doi.org/10.1109/TITB.2006.884369
15. H. Ocak, Automatic detection of epileptic seizures in EEG using discrete wavelet transform and approximate entropy, *Expert Syst. Appl.*, **36** (2009), 2027–2036. https://doi.org/10.1016/j.eswa.2007.12.065
16. J. S. Richman, J. R. Moorman, Physiological time-series analysis using approximate entropy and sample entropy, *Am. J. Physiol. Heart Circ. Physiol.*, **278** (2000), H2039–2049. https://doi.org/10.1152/ajpheart.2000.278.6.H2039
17. Y. Kumar, M. L. Dewal, R. S. Anand, Epileptic seizure detection using DWT based fuzzy approximate entropy and support vector machine, *Neurocomputing*, **133** (2014), 271–279. https://doi.org/10.1016/j.neucom.2013.11.009
18. Y. S. Choi, K. Hyun, J. Y. Choi, Assessing multiscale permutation entropy for short electroencephalogram recordings, *Cluster Comput.*, **19** (2016), 2305–2314. https://doi.org/10.1007/s10586-016-0648-8
19. M. Costa, A. L. Goldberger, C. K. Peng, Multiscale entropy analysis of complex physiologic time series, *Phys. Rev. Lett.*, **89** (2002), 068102. https://doi.org/10.1103/PhysRevLett.89.068102
20. S. D. Wu, C. W. Wu, K. Y. Lee, S. G. Lin, Modified multiscale entropy for short-term time series analysis, *Phys. A*, **392** (2013), 5865–5873. https://doi.org/10.1016/j.physa.2013.07.075
21. Y. Zhang, P. Shang, Refined composite multiscale weighted-permutation entropy of financial time series, *Phys. A*, **496** (2018), 189–199. https://doi.org/10.1016/j.physa.2013.07.075
22. Y. Li, B. Tang, S. Jiao, Q. Su, Snake optimization-based variable-step multiscale single threshold slope entropy for complexity analysis of signals, *IEEE Trans. Instrum. Meas.*, **72** (2023), 6505313. https://doi.org/10.1109/TIM.2023.3317908
23. Y. Li, B. Tang, S. Jiao, Y. Zhou, Optimized multivariate multiscale slope entropy for nonlinear dynamic analysis of mechanical signals, *Chaos Solitons Fractals*, **179** (2024), 114436. https://doi.org/10.1016/j.chaos.2023.114436
24. P. Li, C. Liu, K. Li, D. Zheng, C. Liu, Y. Hou, Assessing the complexity of short-term heartbeat interval series by distribution entropy, *Med. Biol. Eng. Comput.*, **53** (2015), 77–87. https://doi.org/10.1016/j.chaos.2023.114436
25. R. K. Udhayakumar, C. Karmakar, P. Li, M. Palaniswami, Effect of data length and bin numbers on distribution entropy (DistEn) measurement in analyzing healthy aging, in *2015 37th Annual International Conference of the IEEE Engineering in Medicine and Biology Society (EMBC)*, (2015), 7877–7880. https://doi.org/10.1109/EMBC.2015.7320218

26. P. Li, C. Karmakar, C. Yan, M. Palaniswami, C. Liu, Classification of 5-S Epileptic EEG recordings using distribution entropy and sample entropy, *Front. Physiol.*, **7** (2016), 136. https://doi.org/10.3389/fphys.2016.00136
27. D. Y. Lee, Y. S. Choi, Multiscale distribution entropy analysis of heart rate variability using differential inter-beat intervals, *IEEE Access*, **8** (2020), 48761–48773. https://doi.org/10.1109/ACCESS.2020.2978930
28. S. Supriya, S. Siuly, H. Wang, Y. Zhang, Epilepsy detection from eeg using complex network techniques: A Review, *IEEE Rev. Biomed. Eng.*, **16** (2023), 292–306. https://doi.org/10.1109/RBME.2021.3055956
29. É. Lemoine, J. N. Briard, B. Rioux, R. Podbielski, B. Nauche, D. Toffa, et al., Computer-assisted analysis of routine electroencephalogram to identify hidden biomarkers of epilepsy: Protocol for a systematic review, *BMJ Open*, **13** (2023), e066932. https://doi.org/10.1136/bmjopen-2022-066932
30. R. G. Andrzejak, K. Lehnertz, F. Mormann, C. Rieke, P. David, C. E. Elger, Indications of nonlinear deterministic and finite-dimensional structures in time series of brain electrical activity: Dependence on recording region and brain state, *Phys. Rev. E*, **64** (2001), 061907. https://doi.org/10.1103/PhysRevE.64.061907
31. R. G. Andrzejak, K. Schindler, C. Rummel, Nonrandomness, nonlinear dependence, and nonstationarity of electroencephalographic recordings from epilepsy patients, *Phys. Rev. E*, **86** (2012), 046206. https://doi.org/10.1103/PhysRevE.86.046206
32. T. Gautama, D. P. Mandic, M. M. Van Hulle, A differential entropy based method for determining the optimal embedding parameters of a signal, in *2003 IEEE International Conference on Acoustics, Speech, and Signal Processing*, (2023).
33. M. R. Islam, X. Zhao, Y. Miao, H. Sugano, T. Tanaka, Epileptic seizure focus detection from interictal electroencephalogram: A survey, *Cogn. Neurodyn.*, **17** (2023), 1–23. https://doi.org/10.1007/s11571-022-09816-z
34. L. Ilias, D. Askounis, J. Psarras, Multimodal detection of epilepsy with deep neural networks, *Expert Syst. Appl.*, **213** (2023), 119010. https://doi.org/10.1016/j.eswa.2022.119010
35. M. Sunkara, S. R. Reeja, Tri-SeizureDualNet: A novel multimodal brain seizure detection using triple stream skipped feature extraction module entrenched dual parallel attention transformer, *Biomed. Signal Process Control*, **88** (2024), 105593. https://doi.org/10.1016/j.bspc.2023.105593
36. F. Dong, Z. Yuan, D. Wu, L. Jiang, J. Liu, W. Hu, Novel seizure detection algorithm based on multi-dimension feature selection, *Biomed. Signal Process Control*, **84** (2023), 104747. https://doi.org/10.1016/j.bspc.2023.104747
37. L. Jiang, J. He, H. Pan, D. Wu, T. Jiang, J. Liu, Seizure detection algorithm based on improved functional brain network structure feature extraction, *Biomed. Signal Process Control*, **79** (2023), 104053. https://doi.org/10.1016/j.bspc.2022.104053
38. A. Einizade, S. Nasiri, M. Mozafari, S. H. Sardouie, G.D. Clifford, Explainable automated seizure detection using attentive deep multi-view networks, *Biomed. Signal Process Control*, **79** (2023), 104076. https://doi.org/10.1016/j.bspc.2022.104076
39. X. Qiu, F. Yan, H. Liu, A difference attention ResNet-LSTM network for epileptic seizure detection using EEG signal, *Biomed. Signal Process Control*, **83** (2023), 104652. https://doi.org/10.1016/j.bspc.2023.104652

40. D. Lee, B. Kim, T. Kim, I. Joe, J. Chong, K. Min, K. Jung, A ResNet-LSTM hybrid model for predicting epileptic seizures using a pretrained model with supervised contrastive learning, *Sci. Rep.*, **14** (2024), 1319. https://doi.org/10.1038/s41598-023-43328-y
41. T. K. K. Ho, N. Armanfard, Self-supervised learning for anomalous channel detection in EEG graphs: application to seizure analysis, in *Proceedings of the AAAI Conference on Artificial Intelligence*, (2023), 7866–7874. https://doi.org/10.1609/aaai.v37i7.25952

AIMS Press